Section I

Evidence for Site Isolation in Rh-Mo Bimetallic Catalysts Derived from Organometallic Clusters

Research Context

The impetus for the work discussed in this section stems from (i) the proven synergy of Rh-Mo/Al_2O_3 for oxygenate formation and (ii) our working hypothesis in the global investigation of this catalyst system, namely that the Mo serves primarily as a textural promoter and stabilizes site-isolated Rh aggregates. Here, we hope to guarantee the close proximity of the Rh and Mo, and hence enhance the promotional effects of the Mo, in the catalysts derived from binuclear, homogeneous precursors. The catalysts prepared by coadsorption of $RhH(CO)(PPh_3)_3$ and $[Mo(CO)_3Cp]_2$ (molybdenum dimer) were synthesized essentially as control samples having similar chemical features to those in $(PPh_3)_2RhMo(CO)(\mu\text{-}CO)_2Cp$; the monometallic precursors lacked the intimate metal contact–in the form of metal-metal bonds–found in the binuclear precursor. After the H_2 reduction of the catalyst during reactor testing and in transmission infrared studies, the metal-metal bond present in the binuclear precursor may have been disrupted, but the ultimately stable configuration of Rh and Mo in the binuclear-derived materials is indeed influenced by this initial intimate contact as evidenced by the data set forth below. Finally, in the context of discussing the effect of phosphorous in these materials, we highlight the potential to tailor the final properties of a supported metal catalyst through altering the nature of the ligands present on a homogeneous, organometallic precursor.

Section Abstract

The rhodium-molybdenum cluster, $(PPh_3)_2RhMo(CO)(\mu\text{-}CO)_2Cp$, has been employed as a precursor to alumina- and silica-supported catalysts; these catalysts have been applied in CO and CO_2 hydrogenation. When compared to catalysts made from the separate organometallic complexes, $RhH(CO)(PPh_3)_3$ and $[Mo(CO)_3Cp]_2$, the catalysts derived from a binuclear precursor show superior selectivities towards oxygenates for both CO and CO_2 hydrogenation, namely, methanol, dimethyl ether and ethanol. To explore catalytic behavior of the samples more thoroughly, the kinetics of both CO and CO_2 hydrogenation were studied and global activation energies were determined. Fourier transform infrared spectroscopy studies indicate that CO chemisorbs on the cluster-derived catalysts mainly in the form of gem-dicarbonyl while on the catalysts made from separate rhodium and molybdenum complexes it is chemisorbed only in the linear-carbonyl configuration. This gem-dicarbonyl feature in the CO adsorption on the cluster-derived catalysts may imply enhanced site isolation of Rh by Mo.

Introduction

Since Fischer and Tropsch[1,2] reported that CO could be catalytically hydrogenated to a broad range of organic compounds in 1926, great efforts have been made to develop a selective catalytic system to break down the so-called Anderson-Schulz-Flory distribution of the products. With more public attention focused on the reduction of petroleum dependence and on protecting the environment by producing synthetic components for gasoline blends, interest in CO hydrogenation to oxygenates by promoted rhodium catalysts has greatly increased. In contrast to traditional salt-derived bimetallic catalysts, bimetallic cluster-derived catalysts have several potential advantages: specifiable structural characteristics, adjustable metal skeletons, number and/or type of ligands, etc. The continued development of organometallic chemistry offers great opportunities and possibilities in this regard.

Recent investigations in the catalytic chemistry literature have focused on promoted rhodium catalysts with particular emphasis on the promotional effects of molybdenum and on organometallic-derived Rh-Mo catalysts.[3-15] H. Miessner and M. Ichikawa et al.[3-6] have published investigations of bimetallic cluster-derived Rh-Mo catalysts. These cluster-derived catalysts have shown significant oxygenate selectivity in CO hydrogenation when compared with bimetallic catalysts made from metal salts. There are various explanations for the strong promotional effects of the molybdenum on supported rhodium catalysts. Most such explanations tend to attribute the effects to coverage of large rhodium particles by a molybdenum suboxide or to the formation of mixed oxides of rhodium and molybdenum which are thought to be responsible for improved oxygenate selectivity.[5,9,10] This kind of reasoning is probably true when applied to catalysts made from separate metal salts as initial materials and with high metal loading because of the aggregation of the metals during reduction. But this explanation can not account for the result that Rh-Mo bimetallic cluster-derived catalysts have even higher oxygenates selectivity than conventional bimetallic catalysts. The high oxygenate selectivity of such cluster-derived catalysts implies that intrinsic metal-metal interactions present in the catalyst precursor indeed result in different promoting behavior, as reported by Miessner and Ichicawa et al[3-6] as well as this paper. In their most recent paper,[10] Miessner et al. also excluded molybdenum suboxide migration; instead they explained that the Mo promotion results in oxidative disruption of Rh_x particles and prevents the sintering of Rh. By reducing Rh sintering, the catalyst retains a high number of active sites on the boundary of small Rh particles even for the catalysts derived from separate complexes.

Similar structural arguments were put forth by us in earlier work on Rh-Mo catalysts derived from separate rhodium and molybdenum carbonyl precursors.[12] We concluded that the role of molybdenum on alumina was to "site isolate" rhodium in a highly dispersed form that was more proper to oxygenate production than larger rhodium particles. Site isolation can be taken as the limit of ultrahigh dispersion and textural promotion. Based on this investigation of Rh-Mo

bimetallic catalysts, particularly with regard to our infrared spectroscopic results, it seems reasonable to attribute the promotion of rhodium by molybdenum to a site isolation effect which is enhanced by synthesis of the catalyst with an organometallic cluster precursor.

Experimental

The bimetallic cluster, $(PPh_3)_2RhMo(CO)(\mu\text{-}CO)_2Cp$, was synthesized following the method reported by Preston et al.[11] Initial complexes, $RhCl(PPh_3)_3$, $Mo(CO)_6$, NaCp/THF, $RhH(CO)(PPh_3)_3$ and $[Mo(CO)_3Cp]_2$ were purchased from Strem and Aldrich and were used without further purification. Gamma-alumina (American Cyanamid, BET surface area= 250 m^2/g) and Silica (BET surface area=320m^2/g) were heated at 200°C in air for 24 hours before catalyst preparation.

The impregnation method was employed for catalyst preparation. Calculated amounts of cluster or separate complexes were dissolved in dichloromethane and the solution was added to corresponding amounts of support under a N_2 atmosphere. The mixture was then stirred for 2 hours and finally the solvent was removed by vacuum evaporation. The calculated rhodium loading for all the samples presented in this study was 0.5%wt and the samples have a mole ratio of Rh to Mo of 1. Elemental analysis results of the samples are shown in Table 1.

All of the fresh and used catalysts are characterized by CO and H_2 chemisorptions, which are carried out in a classical chemisorption apparatus at room temperature. All of the samples are reduced at 350°C with H_2 flow for 4 hours and degassed at the same temperature under 10^{-5} torr (1 torr = 133.3 Nm^{-2}) for overnight. The chemisorption information of the catalysts can be seen from Table 2.

CO or CO_2 hydrogenation activities of the catalysts were tested in a fixed-bed high pressure reactor. Detailed descriptions of the reactor system, product analysis and pre-treatment of gases can be seen in elsewhere.[12] The reactor was charged with 1.0g of catalyst (approximately

60x100 mesh). The catalyst was oxidized at 200°C in flowing air (30 ml/min) for 4 hours and then reduced at 350°C for 6 hours in flowing H_2 (40 ml/min). After the catalyst reached its stable activity, reaction data were collected at different reaction conditions: 200 to 350°C; 1.0 MPa to 3.0 MPa; CO/H_2 or CO_2/H_2=2 to 0.33; GHSV= 1200 to 2400h^{-1}. Reaction rate is expressed as follow:

$$r = \frac{X \bullet F}{(22414 \bullet 60 \bullet W)} \qquad \text{(mole of CO or } CO_2\text{/gRh/Sec.)}$$

where, X is the conversion of CO or CO_2; F is flow rate of CO or CO_2 (ml/min) at NTP; W is weight (g) of Rh in sample.

The selectivity (S_i) toward product *i* is defined as:

$$S_i = \frac{(n_i \bullet C_i)}{(\Sigma n_i \bullet C_i)}$$

where n_i is the carbon number of the product *i* and C_i is the mole percentage of the component *i* detected.

Based on reaction rates and selectivity data, and their respective temperature dependencies, the natural log of the rate was plotted versus inverse temperature and activation energies for the total reaction and for each product formed were calculated from the slope of the fitted line. To determine the reaction orders for each component with respect to partial pressure of H_2 and CO (or CO_2), the total reaction rate and rates of formation for each product were measured while varying the partial pressure of both H_2 and CO (or CO_2). Total conversions of CO or CO_2 were maintained at less than 7%. These data were fitted by using least-square regression to a linearized power law rate expression as follows:

$$\ln(r_i) = \ln(k_i) + x_i \bullet \ln(P_{H_2}) + y_i \bullet \ln(P_{CO} \text{ or } P_{CO_2})$$

where k_i, x_i and y_i are the rate constant, and rate orders with respect to partial pressure of H_2 and CO (or CO_2), respectively, for the *i* th component.

In situ infrared spectroscopic studies of the catalysts were performed on a Nicolet 510 FT-IR spectrometer using a self-supported sample wafer in an ***in situ*** IR cell. All spectra were recorded at 50 scans with a resolution of 4 cm^{-1}. The mounted wafer was treated in a similar way to the pretreatment of catalyst sample in the reaction tests and then the cell was evacuated at 10^{-3} torr. after this 50 torr of CO was introduced to the wafer at room temperature. IR spectra were recorded after evacuating the IR cell at different temperatures.

Result and Discussion

The positive promotional effect of Mo on supported Rh catalysts for CO hydrogenation motivated us to develop a Rh-Mo cluster-derived catalyst which also includes phosphorous as a possible acidic promoter and/or selective inhibitor. In fact, as the results show Rh-Mo catalysts derived from supported $(PPh_3)_2RhMo(CO)(\mu\text{-}CO)_2Cp$ indeed behave differently from non-cluster-derived catalysts when tested in CO or CO_2 hydrogenation.

CO Hydrogenation Activity and Selectivity

The CO hydrogenation reaction conditions and results are summarized in Table 3. The results indicate that compared with the non-cluster derived catalysts, designated as $Rh,Mo/SiO_2$ and $Rh,Mo/Al_2O_3$, the bimetallic cluster-derived catalysts show superior selectivity towards oxygenates. In addition, the alumina-supported bimetallic cluster shows particularly high activity. Beyond the differences that arise from the different active metal phase precursors, the different supports also seem to alter oxygenate distribution: methanol is the main oxygenate on silica-supported catalysts while a much higher percentage of dimethyl ether is formed on the alumina-supported catalysts compared to other oxygenates. Methanol is dehydrated to dimethyl ether (i.e. dimethyl ether is a secondary product) on alumina-supported catalysts because of the significant Lewis acidity of the alumina surface.

CO_2 Hydrogenation Activity and Selectivity

Table 4 summarizes the reaction conditions and results for CO_2 hydrogenation testing of the catalysts. It can be seen that the activity of the catalysts for CO_2 hydrogenation is lower than that of CO hydrogenation, but again, the cluster-derived catalysts show distinctly higher selectivities toward oxygenates compared with catalysts derived from separate complexes. The differences in the product distributions from those of CO hydrogenation are that methanol is the main oxygenated component for both kinds of oxide-supported catalysts. Nevertheless, dimethyl ether was once again formed on the alumina-supported catalysts. As mentioned above, dimethyl ether is formed by secondary dehydration of methanol and the Lewis acidity of the support drives the dehydration. Therefore, the different dimethyl ether selectivities for CO and CO_2 hydrogenation on the same catalyst should originate from the difference in the basicity of CO and CO_2, i. e. the weak Lewis basicity of CO_2[15] may block some of the Lewis acid sites thereby lowering the rate of dehydration. Another possible reason for the difference in the dimethyl ether formation is related to the reverse water-gas shift reaction. When a mixture of CO_2 and H_2 is fed to the reactor, the CO_2 can undergo the reverse water-gas shift reaction and produce both CO and H_2O. Water formed in this transformation will dissociatively adsorb on the Lewis acid sites of the support surface, and inhibit the dehydration of methanol. In contrast, when CO is fed to the reactor, the water-gas shift equilibrium is driven forward, consuming water which might otherwise inhibit dehydration of methanol, with the result that dimethylether is a more favorable product.

The Effect of Reaction Conditions on Selectivity

Temperature can dramatically change the selectivity of CO and CO_2 hydrogenation on both cluster-derived and mononuclear complex-derived catalysts. Although the changes are similar, the cluster-derived catalysts show higher activity and selectivity to oxygenates at lower temperatures compared with the corresponding mononuclear complex-derived catalysts. Figures 1 and 2 demonstrate the superior performance of the cluster-derived Rh-Mo catalyst by depicting

the product selectivity as a function of temperature. Methanol selectivity, for example, is approximately twice as high (80% compared to 45%) at 250°C over the $RhMo/SiO_2$ than over the $Rh,Mo/SiO_2$.

The reaction rate and oxygenate selectivity increase, and hydrocarbon selectivity decreases, with increasing total pressure. The CO/H_2 or CO_2/H_2 ratio can effect the selectivity of oxygenates although this effect is not as strong as the effect of varying temperature. With higher hydrogen partial pressure, higher oxygenate selectivity is realized. (Fig. 3).

Finally, the cluster-derived catalysts are very stable after break-in (Figure 4), the CO hydrogenation rate and methanol selectivity for $RhMo/SiO_2$ are seen to remain stable for nearly 100 hours on stream.

Apparent Activation Energy of CO or CO_2 Hydrogenation

The apparent activation energy was determined according to the Arrhenus equation,

$$r = k \cdot \exp(\frac{-E_a}{RT})$$

Where, E_a is the apparent activation energy; k is actually the product of the frequency factor of the rate constant, A_o, and the concentration terms maintained constant throughout the experiment. The results for the total reaction and for each product formed from CO and CO_2 hydrogenation are shown in Tables 5 and 6. Here the partial pressure of CO or CO_2 was maintained at approximately 0.5 and CO_x/H_2 ratio was 1.

Generally, apparent activation energy data show good agreement with the activity and selectivity trends implied by the data mentioned above. It can be seen that the global E_a for CO hydrogenation on the cluster-derived catalysts are significantly lower than that on separate complex-derived catalysts. The activation energies for oxygenate formation from CO on cluster-derived catalysts are lower than that of other catalysts. Similarly, for CO_2 hydrogenation, cluster-

derived catalysts exhibit lower global activation energies and significantly lower activation energies for oxygenate formation compared with the other catalysts examined. The most surprising result is the negative energy of activation for oxygenate formation from CO_2. This suggests a very strong heat of adsorption for CO2 on these catalysts. Evidently, promotion by Mo of Rh for CO or CO_2 conversion and oxygenate formation is intrinsically more effective when the catalysts are made from Rh-Mo bimetallic clusters.

Another interesting result from the study of apparent activation energies, which does not appear in the Table 5, is the decline in activation energy for CO hydrogenation on the cluster-derived catalysts with the reaction time during the initial 50 hours on stream. For example, the global activation energy for CO hydrogenation on $RhMo/SiO_2$ decreased from 127 KJ/mol in the 3rd hour on stream to 88 KJ/mol at the 30th hour and stabilized at about 73 KJ/mol thereafter. The mononuclear complex-derived catalysts did not exhibit significant changes in global activation energy with the reaction time. This decrease in global activation energy with time for the cluster-derived catalysts suggests that the nature and number of active sites on this catalyst are transformed in the presence of the reactant gases at reaction conditions. All the E_a data included in the tables are reported when the reaction has reached its stable activity.

Reaction Orders with Respect to Partial Pressure of H_2 and CO or CO_2

In order to obtain the kinetic information for CO or CO_2 hydrogenation related to the total reaction and each component formed, the reaction rates were measured while changing partial pressures of H_2, and CO, or CO_2. Using the least-square regression method, the power law reaction orders were determined from the data and are listed in Tables 7 and 8.

It can be seen from Table 7 that reaction orders with respect to the partial pressure of H_2 are all positive for all components formed and that the reaction orders with respect to CO are mostly negative for hydrocarbon and oxygenate formation in the CO hydrogenation reaction. Although reaction orders of oxygenate formation with respect to H_2 on the cluster-derived catalysts are

slightly lower than that on the mononuclear complex-derived catalysts, the CO inhibition effect on oxygenate formation for the cluster-derived catalysts is significantly weaker than that for the mononuclear complex-derived catalysts. The oxygenate formation rate order with respect to CO is even positive for $RhMo/SiO_2$. Therefore, superior oxygenate selectivity of the cluster-derived catalysts in CO hydrogenation may be explained as the result of weak to zero inhibition of CO or the oxygenate formation rate by chemisorbed on the catalyst surface. Generally, the trends for promotion effects with respect to the partial pressure of H_2 and inhibition effects with respect to the partial pressure of CO on the Rh-Mo bimetallic catalysts reported here are in agreement with the results of the silica-supported Rh, Rh-Fe, Rh-Li, or Rh-Mn catalysts reported by Burch and Petch.[14c]

Similarly, reaction orders with respect to H_2 for all products formed are positive in the CO_2 hydrogenation reaction, with the exception of total reaction and CO formation on $Rh,Mo/Al_2O_3$, where the values are slightly negative. The reaction orders with respect to CO_2 for all product formations are negative. The stronger H_2 and the weaker CO_2 rate dependencies for oxygenate formation on the cluster-derived catalysts compared to that on the mononuclear complex-derived catalysts are in good agreement with the results described.

IR Evidence of Different Surface Features of the Catalysts

Fourier Transform infrared (FTIR) spectra were recorded *in situ* for all catalysts after reduction at 350°C, absorption of CO at 50°C and evacuation at room temperature. The spectra are shown in Figures 5 and 6.

The FTIR spectroscopy study indicates that CO chemisorption on the cluster-derived catalysts leads to mainly the gem-dicarbonyl, while in contrast it leads to principally linear-CO coordination on the mononuclear complex-derived catalysts. This interpretation of the observed IR for chemisorbed CO on these catalysts, is based upon those given by Olive and Olive in their extensive review.[16] Accordingly, a doublet with component peaks at 2101 and 2031 cm^{-1} was

assigned to the symmetric and antisymmetric vibration of dicarbonyls on an isolated Rh species, the broad band at 1855 to 1870 cm^{-1} and the band at 2056 to 2070 cm^{-1} were assigned to bridging CO, ($Rh_2(CO)$), and linear CO, (RhCO) species on more "crystalline" island or rafts of Rh, respectively, in which reduced rhodium atoms form a close-packed array.

The carbonyl absorption characteristics of the IR spectra on the catalysts also show some variation with the oxide support used. For $RhMo/SiO_2$, the strong gem-dicarbonyl absorption appeared at 2103 and 2033 cm^{-1}, broad weak-bridging absorption appeared at 1900 cm^{-1} and almost no linear-CO absorption was observed. In contrast, for $RhMo/Al_2O_3$, there was a distinct linear-CO absorption (2065 cm^{-1}) besides the similar gem-dicarbonyl (2096, 2026 cm^{-1}) and broad weak-bridging (1863 cm^{-1}) CO absorption. These differences in CO absorption are suggestive of the difference in oxygenate distributions on the cluster-derived catalysts supported for the two different oxides. The differences in CO absorption between the mononuclear complex-derived catalysts and the cluster-derived catalysts are evident in both the silica- and alumina-supported cases. Not only were there no gem-dicarbonyl bands on the mononuclear complexes-derived catalysts, but also the linear-CO peak positions are shifted from 2075 cm^{-1} to 2055, 2033 cm^{-1} for $Rh,Mo/SiO_2$, and from 2065 to 2076 cm^{-1} for $Rh,Mo/Al_2O_3$.

It has been reported[5-9] that the gem-dicarbonyl became the main species on the surface of supported rhodium catalysts only when the Mo/Rh ratio is high (>4). The gem-dicarbonyl feature also was thought to be a evidence of a high dispersion of rhodium.[9, 17] However, strong gem-dicarbonyl absorptions were observed on the cluster-derived catalysts in this study, where the Mo/Rh ratio is only 1. After comparison with the IR spectra of mononuclear complex-derived catalysts with the same metal loading, it is evident that the gem-dicarbonyl feature of the cluster-derived catalysts is not a result of low metal loading in this work, though low Rh loading was found to give rise to gem-dicarbonyl on supported Rh catalysts.[16] Therefore, the prominence of the gem-dicarbonyl feature in the CO absorption spectra of the cluster-derived catalysts points to more effective site isolation of rhodium by molybdenum on the alumina and silica surfaces. This

more effective site isolation arise from the fact that after chemisorbing the organometallic precursors, the next step is air oxidation prior to reduction. For the cluster-derived catalysts this is expected to leave more rhodium in the near vicinity of molybdenum than for the mononuclear-complex-derived catalysts for which other surface interactions may lead to less mixing of the metals. Hence due to the strong metal-metal bonds in the cluster precursor, rhodium-molybdenum proximity is maintained and rhodium site isolation is favored in the active form of the catalyst. This special surface feature of the cluster-derived catalysts may correlate to their superior oxygenate selectivity for CO_x hydrogenation.

Effect of Phosphorus

So far, no direct data demonstrate the effect of the presence of phosphorus on the catalysts, but it seems clear that phosphorus could potentially inhibit to some extent the activity of Rh-Mo bimetallic catalysts for CO or CO_2 hydrogenation. Nevertheless, the cluster-derived catalysts indeed show higher activity and superior oxygenate selectivity compared with mononuclear complex-derived catalyst even though both contain phosphorus. Phosphorus present on the surface, while often considered to be an inhibitor to metallic catalysts, may block some active sites on the surface for hydrocarbon formation and could actually decrease hydrocarbon selectivity in favor of oxygenate selectivity. In this way, the inhibitor could provide a useful means to controlling undesired side reactions. The key factor here is that the inhibitor would have to selectively obstruct some of the catalytic sites. Hence molecular modification of the cluster precursor could be a useful means for designing highly selective CO hydrogenation catalysts, not only from the standpoint of specific structural features of metals at the active site, but also from the standpoint of introducing certain ligands in the precursor that would lead to selective inhibitions on the active catalyst. The further development of this kind of surface organometallic chemistry offers some intriguing possibilities for the design of new catalytic materials.[18]

Conclusions

Rh-Mo catalysts derived from the bimetallic cluster, $(PPh_3)_2RhMo(CO)(\mu\text{-}CO)_2Cp$, show higher activity and superior oxygenate-selectivity in the CO and CO_2 hydrogenation reactions compared with catalysts derived from the mononuclear complexes, $RhH(CO)(PPh_3)_3$ and $[Mo(CO)_3(C_5H_5)]_2$. The propensity for oxygenate formation on the cluster-derived catalysts also was confirmed by data derived from apparent activation energies and reaction orders. Gem-dicarbonyl was the main CO-absorbed species on the cluster-derived catalysts, and this implied that rhodium exist as +1 oxidation state. These IR results suggest that effective promotion of Rh by Mo in cluster-derived catalysts for CO hydrogenation might occur through enhanced "site isolation" of Rh by Mo.

Acknowledgments

Support for this research was provided by the Pittsburgh Energy and Technology Center under the auspices of the Department of Energy University Coal Research programs, Grant No. DE-F622-90PC90291.

References

1. F. Fischer and H. Tropsch, *Chem. Ber.*, **59**, (1926)830

2. F. Fischer and H. Tropsch, *Brennst. Chem.*, **7**, (1926)97

3. A. Trunschke, H. Ewald, D. Gutschick, H. Miessner and M. Skupin, B. Walther, and H. C. Bottcher, *J.Mol.Catal.*, **56**, (1989)95.

4. A. Trunschke, H. Ewaald, H. Miessner, A. Fukuoka, and M. Ichikawa, *Mater.Chem.and Phys.*, **29**, (1991)503.

5. A. Trunschke, H. C. Bottcher, A. Fukuoka, M. Ichikawa, H. Miessner, and H. C. Bottcher, *Catal. Lett.*, **8**, (1991)221.

6. R. Lamber , N. I. Jaeger, A. Trunschke, and H. Miessner, *Catal. Lett.*, **11**, 1(1991)1.

7. B. J. Kip, E. G. F. Hermans, J. H. M. C. Van Wolput, N. M. A. Hermans, J. Van Grondelle and R. Prins, *Appl. Catal.* **35**, (1987)109.

8. E. C. DeCanio and D. A. Storm, *J. Catal.* **132**, (1991)375.

9. M. D. Wardinsky and W. C. Hecker, *J.Phys.Chem.*, **92**, (1988)2602.

10. A. Trunschke, H. Ewald and H. Miessner et al., *J.Mol.Catal.*, **74**, (1992)365.

11. L. Carlton, W. E. Lindsell, K. J. McCullough and P. N. Preston, *J.Chem.Soc. Dalton Trans.*, (1984)1693.

12. H. C. Foley, A. J. Hong, J. S. Brinen, L. F. Allard, and A. J. Garratt-Reed, *Appl. Catal.*, **61**, (1990)351.

13. C. Sudhakar, N. A. Bhore, K. B. Bischoff, W. H. Manogue, and G. A. Mills, *Catalysis 1987*, J. W. Ward Ed., Elsevier Sc. Pub., Amsterdam, (1988)115

14. R. Burch and M. I. Petch, (a) *Appl. Catal.* A: **88**, (1992)39. (b) ibid, **88**, (1992)61. (c) ibid, **88**, (1992)77.

15. A. Behr *Carbon Dioxide Activation by Metal Complexes* p15. VCH Verlagsgesellschaft (Germany) 1988.

16. G. Henrici-Olive and S. Olive, *The Chemistry of the catalyzed Hydrogenation of Carbon Monoxide* Page 40. Springer-verlag 1984.

17. J. P. Hindermam, G. J. Hutchings, A. Kiennemann, Catal Review, Sci. Eng., 35(1), (1993)69

18. B. C. Gates, in *Catalyst Design. Progress and Perspectives,* L. L. Hegedus, Ed., Wiley 1987

Table 1. Elemental Analysis of the Rh-Mo Bimetallic Catalysts

Catalysts	% Rh	% Mo	% P	
RhMo/SiO2	0.51	0.47	0.28	
Rh,Mo/SiO2	0.36	0.38	0.25	
RhMo/Al2O3	0.58	0.66	0.39	
Rh,Mo/Al2O3		0.31	0.39	0.33

Note: RhMo and Rh,Mo represent catalysts derived from $RhMo(CO)_3Cp(PPh_3)_2$ and the mixture of $RhH(CO)(PPh_3)_3$ and $[Mo(CO)_3Cp]_2$, respectively.

Table 2. CO and H_2 Chemisorption Data of Rh-Mo Bimetallic Catalysts

Catalysts	State	Condition	CO/Rh	H_2/Rh
RhMo/SiO2	fresh	room temp.	1.06	0.08
	used	"	0.69	0.86
Rh,Mo/SiO2	fresh	"	1.00	0.00
	used	"	0.00	0.00
RhMo/Al2O3	fresh	"	1.19	0.02
	used	"	0.31	0.02
Rh,Mo/Al2O3	fresh	"	1.28	0.28
	used	"	0.66	0.08

Table 3. CO_2-free Selectivity of Rh-Mo Bimetallic Catalysts for CO Hydrogenation

Catalysts	H_2/CO	T°C	P(MPa)	CxHy	MeOH	Me_2O	EtOH	ΣOxy.	r[a]	TON[b]
RhMo/SiO2	2	300	2.0	21.6	73.5	0.3	4.4	78.2	9.80	9.52
Rh,Mo/SiO2	2	300	2.0	48.0	41.5	/	10.5	52.0	12.5	12.9
RhMo/Al2O3	2	250	1.87	24.8	17.8	44.9	12.4	75.1	55.2	47.8
Rh,Mo/Al2O3	2	300	2.0	37.4	19.9	42.7	/	62.5	3.87	3.11

a. Total reaction rate in the unit of 10^{-6}xMol CO/gRh/Sec.

b. Turnover frequency, in the unit of 10^{-4}/sec, calculated from CO chemisorption data.

Table 4. CO-free Selectivity of Rh-Mo Bimetallic Catalysts for CO_2 Hydrogenation

Catalysts[a]	H_2/CO_2	T°C	P(MPa)	CxHy	MeOH	Me_2O	EtOH	ΣOxy.	r[b]	TON[c]
RhMo/SiO2	1	300	2.0	36.3	61.9	/	1.9	63.8	1.75	1.70
Rh,Mo/SiO2	1	350	2.0	59.5	39.5	/	1.0	40.5	3.47	3.57
RhMo/Al2O3	1	300	2.0	43.4	44.1	8.7	3.9	56.6	1.72	1.49
Rh,Mo/Al2O3	1	350	2.0	55.8	43.0	1.2	/	44.2	3.10	2.50

a. The catalysts are same with table 1.

b. Total reaction rate in the unit of 10^{-6}xMol CO_2/gRh/Sec.

c. Turnover frequency in the unit of 10^{-4}/sec, calculated from CO chemisorption data.

Table 5. Apparent Activation Energy of $CO+H_2$ on Bimetallic Catalysts (KJ/mol)

	$RhMo/SiO_2$	$Rh,Mo/SiO_2$	$RhMo/Al_2O_3$	$Rh,Mo/Al_2O_3$
Total reaction	73	93	85	102
CH_4	92	104	129	129
C_2H_6	100	105	152	122
C_3H_8	88	100	133	113
C_4H_{10}		108	123	83
MeOMe			63	67
MeOH	60	66	78	79
EtOH	56	71	69	

Table 6. Apparent Activation Energy of CO_2+H_2 on Bimetallic Catalysts (KJ/mol)

	$RhMo/SiO_2$	$Rh,Mo/SiO_2$	$RhMo/Al_2O_3$	$Rh,Mo/Al_2O_3$
Total reaction	54	68	64	67
CO	54	68	66	67
CH_4	90	89	105	93
C_2H_6	92	111	92	84
C_3H_8	97	120	96	85
MeOMe	-17		-27	-31
MeOH	-24	19	-4.2	19
EtOH			-32	

Table 7. CO Hydrogenation Reaction Orders

Products	$RhMo/SiO_2$	$Rh,Mo/SiO_2$	$RhMo/Al_2O_3$	$Rh,Mo/Al_2O_3$
Reaction orders with respect to H_2				
Total	0.54	0.73	0.08	0.06
CO_2	0.49	0.84	0.01	0.33
CH_4	0.75	0.97	0.76	0.81
C_2H_6	0.47	0.55	0.73	0.56
C_3H_8	0.42	0.53	0.61	0.09
C_4H_{10}	0.26		0.08	
MeOMe			0.96	1.36
MeOH	0.73	1.15	0.69	0.76
EtOH	0.82	0.77	0.50	
Reaction orders with respect to CO				
Total	0.68	0.06	-0.11	-0.35
CO_2	0.83	0.69	0.08	0.59
CH_4	-0.48	-0.29	-0.76	-0.25
C_2H_6	-0.33	-0.17	-0.27	-0.14
C_3H_8	0.07	0.03	0.36	0.48
C_4H_{10}	-0.45		0.49	
MeOMe			-0.84	-0.76
MeOH	0.49	-0.35	-0.24	-1.54
EtOH	0.37	-0.55	-0.94	

Table 8. CO_2 Hydrogenation Reaction Orders

Products	$RhMo/SiO_2$	$Rh,Mo/SiO_2$	$RhMo/Al_2O_3$	$Rh,Mo/Al_2O_3$
Reaction orders with respect to H_2				
Total	0.46	0.3	0.29	-0.31
CO	0.28	0.3	0.29	-0.40
CH_4	0.49	0.55	0.79	0.66
C_2H_6	0.54	0.73	0.21	0.14
C_3H_8	0.43	1.30	0.45	0.62
MeOMe			0.89	1.35
MeOH	0.35	1.42	0.35	1.23
EtOH	-0.47		0.36	
Reaction orders with respect to CO_2				
Total	-0.06	-0.22	-0.13	-0.61
CO	-0.21	-0.22	-0.11	-0.68
CH_4	-0.85	-1.30	-0.47	-0.80
C_2H_6	-0.34	-1.50	-0.55	-1.42
C_3H_8	-0.19	-1.76	0.25	-0.81
MeOMe			-1.84	-2.8
MeOH	-1.27	-1.67	-1.15	-0.81
EtOH	-1.74		-0.42	

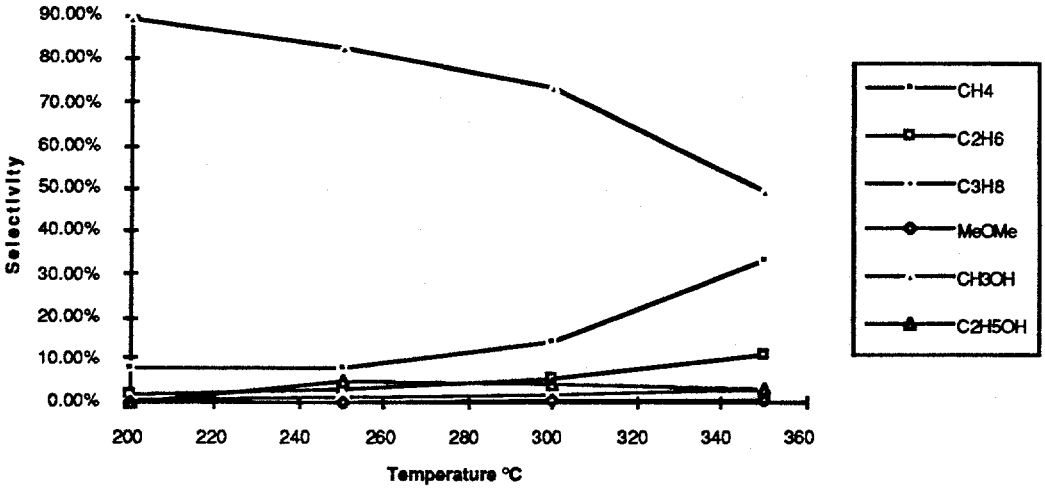

Figure 1. Temperature dependences of selectivities on RhMo/SiO2 (300psi, CO/H2=1/2).

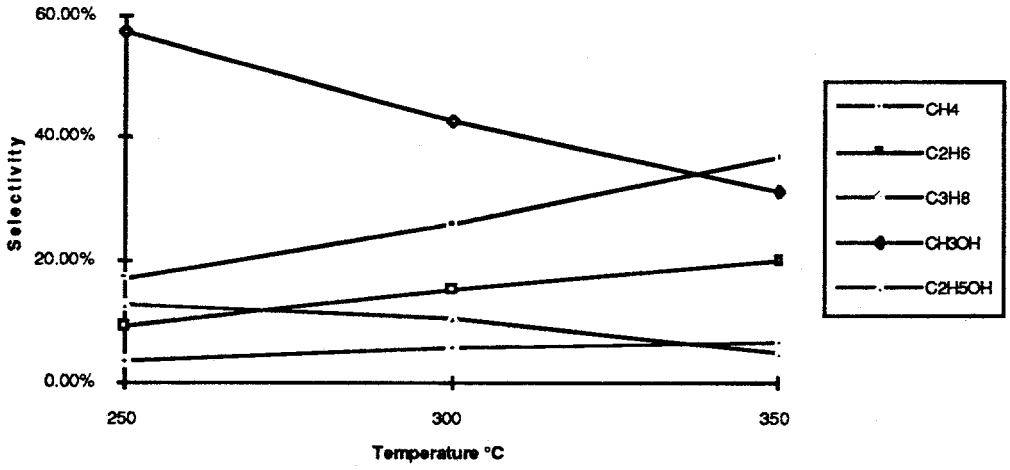

Figure 2. Temp. dependences of selectivities of Rh,Mo/SiO2. (300psi, CO/H2=1/2).

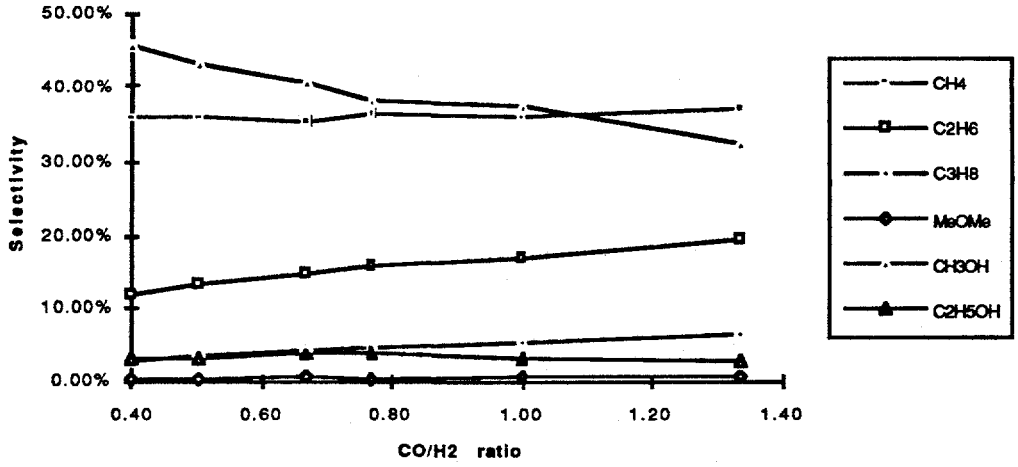

Figure 3. Effect of CO/H2 ratio on selectivity (RhMo/SiO2, 350°C, 300psi).

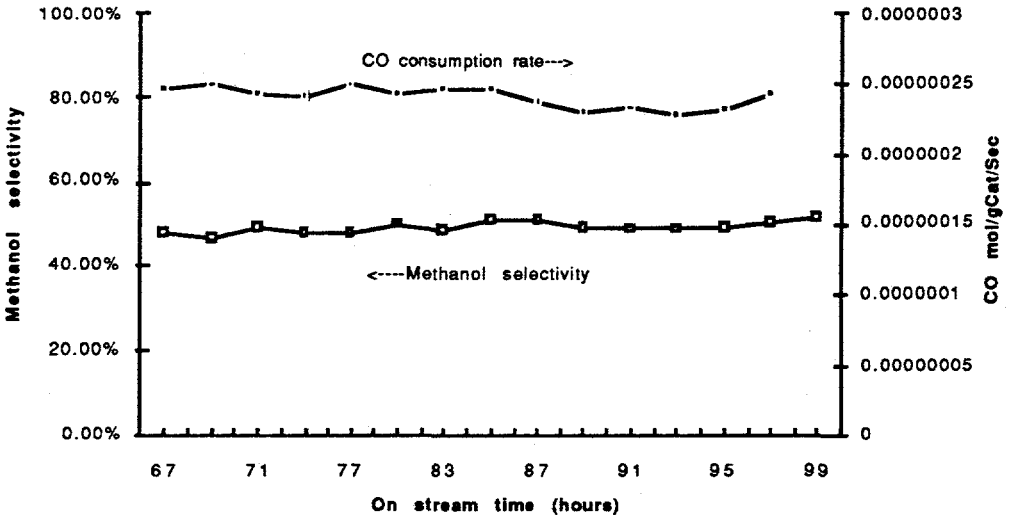

Figure 4. Stability of RhMo/SiO2 (350°C, 300psi, CO/H2=1/2).

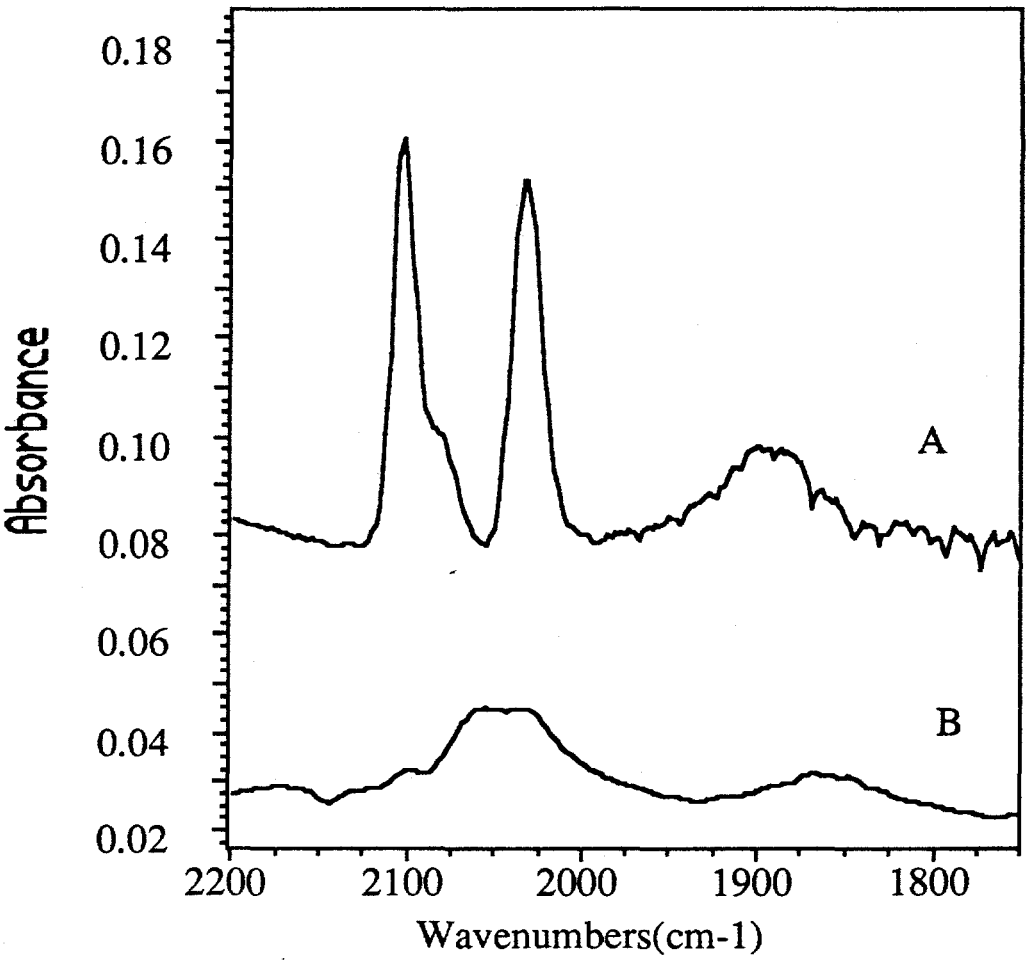

Fig. 5 A: CO-absorbed RhMo/SiO2 evacuated at RT
B: CO-absorbed Rh,Mo/SiO2 evacuated at RT

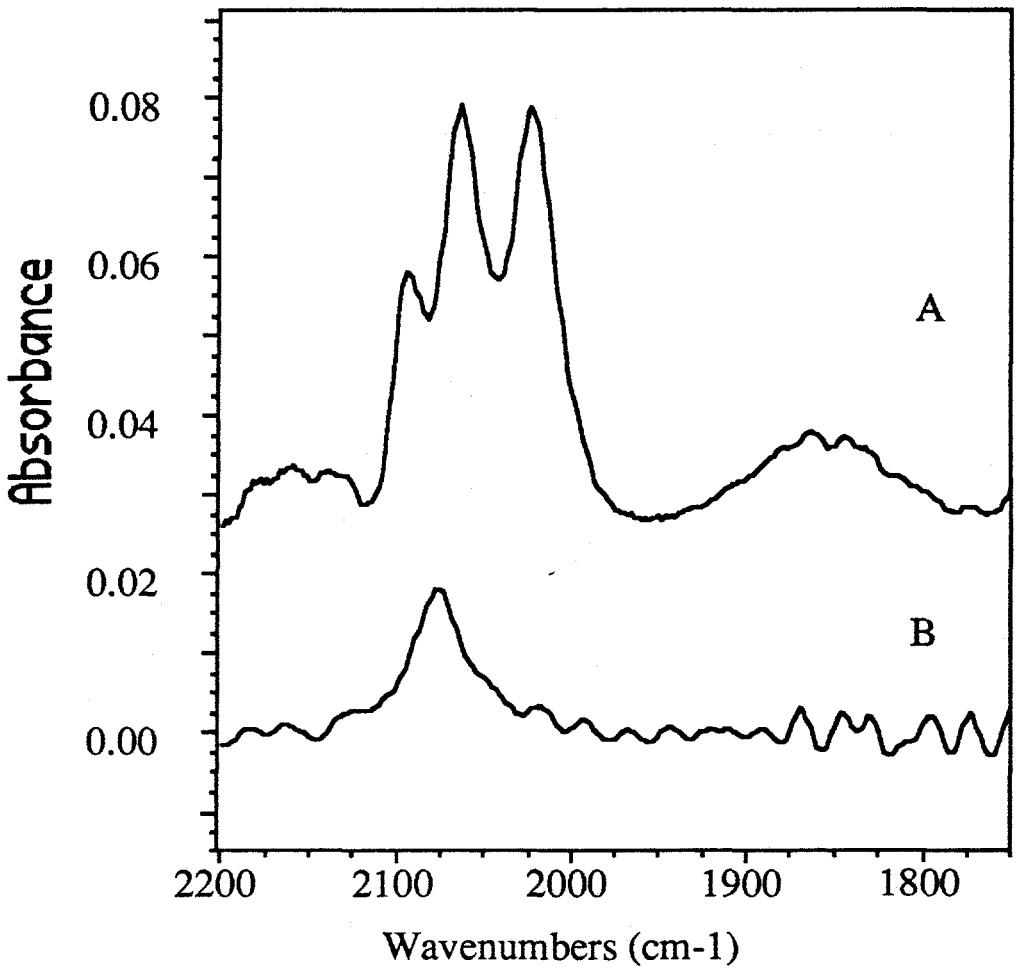

Fig. 6 A: CO-absorbed RhMo/Al2O3 evacuated at RT.
B: CO-absorbed Rh,Mo/Al2O3 evacuated at RT.